

# An LSTM-Aided Hybrid Random Access Scheme for 6G Machine Type Communication Networks

Wenchao Zhai, Huimei Han, Lei Liu, Jun Zhao

**Abstract**—In this paper, an LSTM-aided hybrid random access scheme (LSTMH-RA) is proposed to support diverse quality of service (QoS) requirements in 6G machine-type communication (MTC) networks, where massive MTC (mMTC) devices and ultra-reliable low latency communications (URLLC) devices coexist. In the proposed LSTMH-RA scheme, mMTC devices access the network via a timing advance (TA)-aided four-step procedure to meet massive access requirement, while the access procedure of the URLLC devices is completed in two steps coupled with the mMTC devices' access procedure to reduce latency. Furthermore, we propose an attention-based LSTM prediction model to predict the number of active URLLC devices, thereby determining the parameters of the multi-user detection algorithm to guarantee the latency and reliability access requirements of URLLC devices. We analyze the successful access probability of the LSTMH-RA scheme. Numerical results show that, compared with the benchmark schemes, the proposed LSTMH-RA scheme can significantly improve the successful access probability, and thus satisfy the diverse QoS requirements of URLLC and mMTC devices.

**Index Terms**—LSTM, mMTC, quality of service, random access, URLLC.

## I. INTRODUCTION

WITH the rapid development of the Internet of Things (IoT) industry, such as smart cities and autonomous driving, the amount of data generated by machine-type communication (MTC) accounts for a great proportion in all communication services [1], [2]. The fifth-generation (5G) communication standard has defined two types of services for MTC [3]: one is massive machine type communications (mMTC), which aims to provide massive connections; the other is ultra-reliable low latency communications (URLLC), which

focuses on supporting high reliability and low latency communications. However, the key performance indicators of 5G are not enough to meet some future MTC requirements [4], such as the 5G air interface delay (less than 1 ms) is difficult to meet the haptic internet-based telemedicine air interface delay (less than 0.1 ms). To tackle these problems, several research projects around the world have recently studied the next generation mobile communication systems, namely the sixth generation mobile communication systems (6th-Generation, 6G) [5], [6].

Compared with 5G, the 6G communication systems will achieve lower power consumption, lower latency, higher reliability, and so on. Thus, 6G will become the main force to support and promote IoT services in the future, bringing performance benefits and unprecedented services to users [5]. According to the prediction of Cisco visual networking index, the number of MTC devices will be around 28.5 billion by 2022 [7]. MTC will be a critical cornerstone for the future 6G systems due to the requirement of vertical-specific wireless network solutions. Furthermore, many MTC applications in 6G will encompass both URLLC and mMTC services, whereas mMTC and URLLC have been often studied separately in 5G [8].

Random access procedure, initiating the data transmission, is a critical step in 6G communication systems [8]. The design of random access schemes for the MTC network has attracted much attention in recent years. The third generation partnership project (3GPP) has proposed several congestion control approaches to decrease the network load in the random access procedure, thereby improving the uplink throughput [9]. The popular one is access class barring (ACB) based methods where devices whose generated random values are less than or equal to the ACB factor can access the network. Several enhanced ACB-based random access schemes were proposed, such as dynamic-ACB-based schemes [10], [11], cooperative-ACB-based scheme [12], and joint ACB and timing advance (TA) based scheme [13]. Moreover, other congestion control strategies, such as slotted/backoff based approaches, were also described in [9]. Considering

Wenchao Zhai is with the China Jiliang University, Hangzhou, Zhejiang, 310018, P.R. China, Huimei Han is with College of Information Engineering, Zhejiang University of Technology, Hangzhou, Zhejiang, 310032, P.R. China, Lei Liu is with the State Key Lab of Integrated Services Networks, Xidian University, Xi'an, 710071, P.R. China, and Jun Zhao is with School of Computer Science and Engineering, Nanyang Technological University, Singapore. (Email: zhaiwenchao@cju.edu.cn, hmhan1215@zjut.edu.cn, tianjiaoliulei@163.com, junzhao@ntu.edu.sg)

the small data packet transmission of MTC devices, to reduce the signaling overhead, Laya *et al.* proposed to transmit the data information of MTC devices during MSG1 or MSG3 transmission stage [14]. The above-mentioned schemes are orthogonal random access (ORA) schemes, where each resource block can only be allocated to a single MTC device. This will decrease data transmission efficiency, reduce resource utilization and the number of successful devices, as well as increase the access delay and energy consumption.

The non-orthogonal random access (NORA) schemes, which allows multiple MTC devices share the same resource block to overcome the drawbacks of ORA, attracted much attention in recent years. Seo *et al.* proposed a power-domain non-orthogonal multiple access based random access scheme, where multi-channel selection diversity is utilized to improve the energy efficiency [15]. Shirvanimoghaddam *et al.* proposed a rateless analog fountain code based NORA scheme, where MTC devices are grouped based on their delays, and devices from the same group transmit their uplink messages to the BS via the same resource block [16]. Liang *et al.* proposed a power domain based NORA scheme, where MTC devices transmit their uplink messages with different transmitting powers via the same resource block, and the BS recovers the uplink message of each device by employing a successive interference cancellation (SIC) algorithm [17]. Considering sparse activity of MTC devices, the problem of detecting uplink message can be transformed into the problem of sparse signal recovery in compressed sensing. Then, the BS performs active MTC device detection, channel response estimation, and uplink message decoding by utilizing a measurement matrix [18], [19]. Ahn *et al.* proposed a Bayesian-based random access scheme for the case of the BS with a single antenna, where an expectation propagation algorithm is utilized to perform activity detection and channel estimation jointly [18]. Liu *et al.* proposed an approximate message passing (AMP) based grant-free scheme to solve the massive access problem in massive MIMO systems [19]. Machine learning has strong learning and expression capabilities and has been widely used in communications [20]–[22]. Researchers conduct research on machine learning based NORA scheme in the past few years. Luis *et al.* proposed a reinforcement learning based NORA scheme [20]. In this scheme, ACB parameters are used as reinforcement learning actions, the number of collision-free preambles is used as the reward value of reinforcement learning, and the ACB parameter values under the different number of active devices are learned. Gui *et al.* proposed a long short-term memory (LSTM)-based NORA scheme where an LSTM-based deep learning model is utilized to learn the channel characteristics between the BS and the device for

better power allocation, and then the multi-user detection technology is used for uplink message decoding [21]. Ye *et al.* established an end-to-end NORA network model, where deep variational autoencoder is utilized to realize the uplink message decoding and active UE detection [22]. However, the above studies only have considered the case of all devices having the same priority, which are not suitable for MTC network with diverse quality of service (QoS) in 6G [8].

To solve this problem, Weerasinghe *et al.* proposed a group-based random access scheme, where URLLC devices are grouped and some preambles are preserved for these devices, whereas mMTC devices still utilize the traditional orthogonal access mechanism. However, the traditional orthogonal access mechanism cannot meet the requirements of massive connections of mMTC devices, leading to network congestion [23]. Qi *et al.* proposed a multi-channel ALOHA random access scheme. This scheme divides the channel resources in the time domain and the frequency domain to obtain multiple sub-channel resources, and provides more access resources for URLLC devices to ensure the low-latency and high-reliability connection of URLLC devices. However, when multiple devices send uplink messages via the same sub-channel, this scheme cannot decode the uplink messages of these devices, and thus limits the number of successful access devices [24].

To guarantee diverse QoS requirements in 6G MTC networks where URLLC and mMTC devices coexist, we propose an LSTM-aided hybrid random access (LSTMH-RA) scheme. In the proposed LSTMH-RA scheme, mMTC devices access the network via a TA-aided four-step procedure, while the access procedure of the URLLC devices is completed in two steps coupled with the mMTC devices' access procedure. Furthermore, we propose an attention-based LSTM prediction model to predict the number of active URLLC devices, thereby determining the parameters of the multi-user detection algorithm to guarantee the latency and reliability access requirements of URLLC devices. The **main contributions** of this paper are summarized as follows<sup>1</sup>.

- 1) We propose an attention-based LSTM prediction model to predict the number of active URLLC devices. Thus, the BS can determine the parameters of multi-user detection dynamically to meet the reliability requirement. Furthermore, this also ensures that almost all URLLC devices can access the network in one shot to satisfy the latency requirement.
- 2) We utilize the SIC algorithm in power domain to decode the uplink message of mMTC devices. **The SIC algorithm decodes the uplink messages of mMTC**

<sup>1</sup>Since we have also uploaded this paper to arXiv, the arXiv paper [25] is the same as this paper.

devices from the highest to the lowest power level. As long as mMTC device with the highest power level experiences power collision, other mMTC devices with/without power collision will not be successfully decoded. To enable other mMTC devices without power collision have opportunity to be decoded successfully, we propose to allocate the highest power level to mMTC devices experiencing no TA collision with contenders selecting the same preamble, and allows other mMTC devices to randomly select their power levels.

- 3) We analyze the successful access probability of the proposed LSTMH-RA scheme. Numerical results show that the simulation results accord well with the analytical results. In addition, compared with the benchmark schemes, the proposed scheme significantly improves the successful access probability, and thus satisfies the diverse QoS requirements of URLLC and mMTC devices.

The remainder of this paper is organized as follows. Sections II and III introduce the system model and the proposed LSTMH-RA scheme, respectively. In Section IV, we analyze the performance of the proposed LSTMH-RA scheme. Sections V and VI provide numerical results and conclusions, respectively.

**Notation.** Table I describes the notations utilized throughout this paper.

TABLE I  
NOTATIONS.

Notations	Description
$(\cdot)^T$	The transpose operation of a vector or a matrix
$ \cdot $	The cardinality of a set
$\text{concat}(\cdot)$	The concat function
$\exp(\cdot)$	The exponential function
$\mathcal{CN}(\mu, \sigma^2)$	A circularly-symmetric complex Gaussian distribution with mean $\mu$ and variance $\sigma^2$
$\tanh(\cdot)$	The hyperbolic tangent function
$ a $	The modulus of complex number $a$
$\lceil \cdot \rceil$	Round up to an integer
$\mathcal{P}(\lambda)$	Poisson distribution with parameter $\lambda$
$\mathcal{B}(b, c)$	Binomial distribution with parameters $b$ and $c$
$\otimes$	Circular convolution operation
$[\mathbf{d}]_i$	The $i^{\text{th}}$ element of vector $\mathbf{d}$
$\mathbb{C}$	The complex numbers space

## II. SYSTEM MODEL

In this paper, we consider a cell with radius of  $R$ , where a BS is in the center of the cell and all  $K$  devices (i.e., mMTC devices and URLLC devices) are uniformly distributed in the cell, as shown in Fig. 1. Furthermore, the BS is equipped with  $M$  antennas and each device has a single antenna. The number of the active devices is  $N_a$ , including  $N_U$  URLLC devices and  $N_M$  mMTC devices, and there are  $\tau_p$  available preambles. **In addition, we consider the block fading channel, and the system is**

in the time division duplex (TDD) mode. Similar to [26], the steps of the proposed LSTMH-RA scheme are performed in a single coherence interval, and the downlink channel can be estimated via the uplink pilots due to the channel reciprocity [27].

We utilize the SIC algorithm in power domain to decode the uplink message of each mMTC device. To improve the performance of the SIC algorithm, we propose to allocate the highest power level to mMTC devices experiencing no TA collision with contenders selecting the same preamble, and allows other mMTC devices to randomly select their power levels. Next, we first introduce the TA information, and then describe the power levels.

The TA information is an index value after quantizing its round-trip propagation delay with the granularity of  $d = 16T_s \times c$  [28]. Thus, the maximum TA value is  $\zeta = \lceil \frac{2R}{d} \rceil$ . Apparently, MTC devices in each annulus obtained by quantizing distance  $d/2$  from the center to the edge of the cell, have the same TA information [28] as shown in Fig. 1. We use  $TA_i$  to denote the TA index of devices located at the  $i^{\text{th}}$  annulus. For example, as shown in Fig. 1, TA indexes of mMTC devices n1, n2, n3 and n4 are  $TA_1, TA_1, TA_2$ , and  $TA_3$ , respectively. Furthermore, each mMTC device can know its distance to the BS via distance measuring technologies, and thus obtains its TA information [29]. For the case of mMTC devices n1, n2, n3 and n4 selecting the same preamble, n3 and n4 are TA collision-free mMTC devices.

In addition, the SIC algorithm decodes the uplink message of each mMTC device from the highest to the lowest power levels. Consider that there are  $L$  power levels, denoted by  $\{l_1, \dots, l_j, \dots, l_L\}$  satisfying  $l_1 > \dots > l_L$ , and  $l_j$  ( $j = 1, \dots, L$ ) is written as [30]

$$l_j = \gamma(\gamma + 1)^{L-j}, \quad (1)$$

where  $\gamma$  is the target signal to interference plus noise ratio (SINR).

## III. THE LSTMH-RA SCHEME

### A. The LSTMH-RA Scheme Description

Fig. 2 illustrates the proposed LSTMH-RA scheme, which aims at meeting the diverse QoS requirements in 6G MTC networks. Specifically, mMTC devices access the network via a timing advance (TA)-aided four-step procedure to meet massive access requirement, while the access procedure of the URLLC devices is completed in two steps coupled with the mMTC devices' access procedure to reduce latency. Furthermore, we propose an attention-based LSTM prediction model to predict the number of active URLLC devices, thereby determining the parameters of the multi-user detection algorithm to

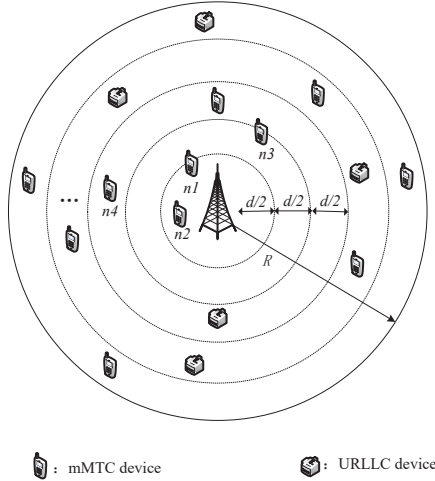


Fig. 1. System model.

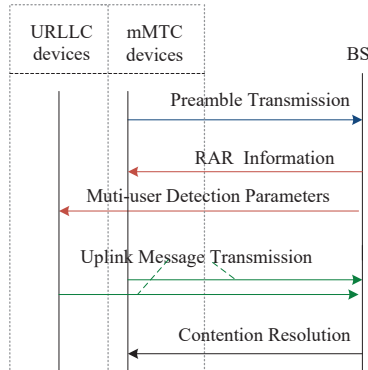


Fig. 2. The proposed random access procedure.

guarantee the latency and reliability access requirements of URLLC devices. The details are described as follows.

### Step 1: Preamble Transmission

Each active mMTC device randomly selects a preamble sequence from the preambles pool  $\mathbf{P}_o = \{\phi_1, \dots, \phi_t, \dots, \phi_{\tau_p}\}$  where  $\phi_t$  is a Zadoff-Chu (ZC) sequence with length  $L_p$  [31] and  $\tau_p$  is the number of preambles. Note that, to overcome the propagation delay, the cyclic prefix (CP) is usually added as the head of preamble sequence.

Let  $\rho_k^p$  denote the preamble transmitting power, and  $b(k)$  be the index of preamble selected by device  $k$ . Let  $\mathbf{h}_k = \sqrt{\beta_k} \mathbf{g}_k \in \mathbb{C}^{M \times 1}$  denote the channel state information (CSI) between device  $k$  and the BS, where  $\beta_k$  denotes the large scale fading parameter which can be known for device  $k$  [32] and  $\mathbf{g}_k$  is the small scale fading with each element in  $\mathbf{g}_k$  having a distribution of  $\mathcal{CN}(0, 1)$ .

Then, the received preamble signal  $\mathbf{Y}$  is given by

$$\mathbf{Y} = \sum_{i=1}^{\zeta} \sum_{k \in \mathcal{A}_i} \sqrt{\rho_k^p \beta_k} \mathbf{g}_k (\phi_{b(k), i})^T + \mathbf{N}, \quad (2)$$

where  $\mathbf{N} \in \mathbb{C}^{M \times L_p}$  stands for the additive complex Gaussian white noise matrix with each element having a distribution of  $\mathcal{CN}(0, \sigma^2)$ , and  $\phi_{b(k), i} \in \mathbb{C}^{L_p \times 1}$  is obtained by cyclically shifted  $i-1$  symbols from preamble sequence  $\phi_{b(k)}$  due to the propagation delay [28]. We utilize power control  $\rho_k^p \beta_k = 1$  to make all preambles have the same received power. In addition, each mMTC device should also transmit its identification (ID) information to the BS, to facilitate the BS to detect the collision-free devices.

### Step 2: Random Access Response (RAR) Transmission and Multi-User Detection Parameters Broadcasting

Through performing the circular convolution operation on the received preamble signal  $\mathbf{Y}$  and preamble sequence  $\phi_t$ , the  $i^{th}$  element is given by [28]

$$\mathbf{y}_{t,i} = \left[ \mathbf{Y} \otimes \frac{\phi_t^*}{\|\phi_t\|} \right]_i = \sqrt{L_p} \sum_{m \in \mathcal{C}_{t,i}} \mathbf{g}_m + \mathbf{N}, \quad (3)$$

where  $\mathcal{C}_{t,i}$  denotes the set of devices selecting preamble  $\phi_t$  in the  $i^{th}$  annulus.  $|\mathcal{C}_{t,i}| = 1$  means that the mMTC device selecting  $\phi_t$  in the  $i^{th}$  annulus is free from TA collision, and thus the BS can successfully decode the ID information of this mMTC device. In other words, the BS can identify mMTC devices with TA collision-free. Then, the BS generates a RAR for each TA collision-free mMTC device, mainly including preamble identification  $t$ , TA index, and resource blocks.

Then, the BS predicts the number of active URLLC devices via utilizing our proposed attention-based LSTM prediction model, which is described in Section II-B. Given the predicted number of active URLLC devices and the channel environment, the BS determines the parameters of multi-user detection (including the resource block, modulation and code schemes), and **the BS broadcasts a pilot followed by the multi-user detection parameters via the broadcast channel, where the broadcasted pilot is known to all active devices.**

### Step 3: Uplink Message Transmission

Based on the received RARs, each mMTC device first finds RARs corresponding to its selected preamble, and then matches the TA information in these RARs with its own. If the TA information contained in one RAR is the same as its own, it selects the highest power level  $l_1$ , and utilizes it to obtain the transmitting power of uplink message according to  $\frac{l_d}{\beta_k}$ . Otherwise, this mMTC device randomly selects a resource block from resource blocks corresponding to its selected preamble, randomly selects a power level (denoted by  $l_d, d = 2, \dots, L$ ), and transmits its uplink message with transmitting power  $\frac{l_d}{\beta_k}$ .

via the selected resource block. Note that, the uplink message of each mMTC device is encoded by the low-density parity-check (LDPC) code according to the 3GPP specification [33].

In addition, using the received pilot signal, each URLLC device estimates its channel state information and thus obtains the multi-user detection parameters by correlating the received message with the estimated channel state information. Then, based on the broadcasted parameters of multi-user detection, each URLLC device modulates and encodes its payload data to obtain its uplink message, and transmits it to the BS via the allocated resource block.

#### Step 4: Contention Resolution

The BS utilizes the SIC algorithm in power domain to detect the received uplink message in each resource block allocated to mMTC devices. The SIC algorithm decodes the uplink messages of mMTC devices from the highest to the lowest power level. The following two events ensure that a device selecting power level  $l$  can be successfully decoded [30]: 1) this device is free from power collision and the messages from devices with power levels larger than  $l$  are successfully decoded; 2) this device is free from power collision and the number of devices with power levels larger than  $l$  is zero. If the messages from this device can be decoded successfully, the interference of the uplink message of this device will be cancelled from the received uplink message. Otherwise, this device fails to access the network and will access the network in the upcoming random access time slot.

The BS decodes the uplink messages of URLLC devices via using the multi-user detection algorithm, which is not the focus of our paper and readers who are interested in this can refer to papers [34]–[36] and references therein. The coding and modulation schemes can be adjusted to satisfy the reliability requirement of URLLC devices based on the number of active URLLC devices [34]–[36]. If the predicted number of URLLC devices is less than the actual value, we assume that all URLLC devices cannot be successfully decoded due to the incorrect coding and modulation schemes. Section III-C will show that, the probability of such an event is really small. Note that, if the BS successfully decodes the uplink message of one device, the BS will send ACK information to this device. Thus, the device can realize that its uplink message has been successfully detected.

In addition, in the proposed LSTMH-RA scheme, mMTC devices access the network via a TA-aided four-step procedure to meet massive access requirement, while the access procedure of the URLLC devices is completed in two steps coupled with the mMTC devices' access procedure to reduce latency. The BS does not need to know the number of active mMTC devices for

the access procedure of mMTC devices, and the BS predicts the number of active URLLC devices via utilizing our proposed attention-based LSTM prediction model for the access procedure of mMTC devices. Thus, the proposed LSTMH-RA scheme can be used in practice. Furthermore, for mMTC devices, the proposed access procedure consumes two round-trip process. From the procedure of the proposed scheme, we observe that, the delay depends largely on step 4 of the proposed access procedure because the BS needs to decode the uplink message of active mMTC device during this step. Fortunately, the demodulation chip achieves lower demodulation delay. Hence, the proposed scheme will cause a lower delay for mMTC devices. In addition, most mMTC devices is in low/no mobility [3]. Due to the fact that the device's speed is inversely proportional to the coherence time, the proposed scheme can be used for mMTC devices.

*Remark 1 (What happens to the extremely overloaded network):* In the proposed LSTMH-RA scheme, if mMTC devices selecting the same preamble can be distinguished by utilizing the TA information, the BS will allocate resources to these distinguished TAs corresponding to these distinguished mMTC devices. Then, only distinguished mMTC devices will utilize the highest power level to transmit their uplink messages via the allocated resources corresponding to their TAs. By doing so, the BS utilizes the SIC algorithm to successfully decode the uplink messages of these distinguished mMTC devices. Otherwise, the mMTC device will randomly select a resource block from resource blocks corresponding to its selected preamble and randomly select a power level to transmit its uplink message. Hence, when the network is extremely overloaded, the probability that mMTC devices selecting the same preamble but having different TA information will be very low, leading to the increase of power collision for the devices whose TA information cannot be distinguished. As a result, the throughput of the proposed LSTMH-RA scheme will be low. To solve this problem, the access class barring (ACB) mechanism [9] can be utilized to reduce traffic overload as in [32]. More specifically, the BS broadcasts ACB factor before step 1 of the proposed LSTMH-RA scheme. Then, mMTC devices passing the ACB check will perform the LSTMH-RA procedure.

#### B. Attention-based LSTM prediction model

To ensure the reliability requirement of URLLC device, our proposed random access scheme predicts the number of active URLLC devices during each random access time slot. Convolutional Neural Network (CNN) and LSTM are two generally used deep-learning models, where CNN is mainly used to handle image data and LSTM is usually used for sequential data [37]. The

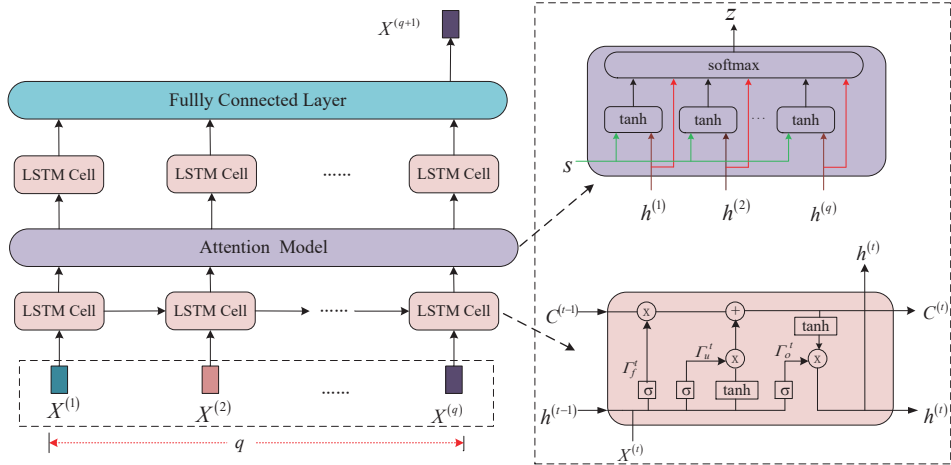


Fig. 3. An attention-based LSTM prediction model consisting of two LSTM layers, one attention layer and one fully connected layer.

number of URLLC devices follows Poisson distribution, and can be considered as sequential inputs. In addition, attention mechanism is a useful tool to improve the performance of the LSTM model [38]. Hence, we use the attention-based LSTM prediction model.

This prediction model consists of two LSTM layers, one attention layer and one fully connected layer, as shown in Fig. 3. The data set are the input of the first LSTM layer, and the outputs of the first LSTM layer are fed into the attention layer. Then, we take the output of the attention layer as the input of the second LSTM layer, and the output of the second LSTM layer is connected to a fully connected layer to predict the number of active URLLC devices. Our training data is the number of URLLC devices from  $t + 1$  to  $t + q$ , which are generated based on the distribution model of URLLC devices. Furthermore, to ensure the reliability and latency requirements of URLLC devices, we take the maximum number of active URLLC devices from  $t$  to  $t + d$  random access time slots as the possible value in the  $t^{th}$  random access time slot. In the following, we describe this prediction model in detail.

1) *LSTM layer*: The powerful ability in preserving temporal memory makes LSTM inherently advantageous to perform the prediction task. Each LSTM layer consists of multiple LSTM cells. An LSTM cell consists of three kinds of gates, namely input gate, output gate, and forget gate. The input data of the first LSTM layer is  $\mathbf{X} = [X^{(1)}, X^{(2)}, \dots, X^{(q)}]$ , where  $q$  is the length of input. The process of building gates during the  $t^{th}$  time step is

given by [39]

$$\begin{cases} \Gamma_f^{(t)} = \delta(W^{(f)}[h^{(t-1)}, X^{(t)}] + b^{(f)}) \\ \Gamma_u^{(t)} = \delta(W^{(u)}[h^{(t-1)}, X^{(t)}] + b^{(u)}) \\ \tilde{C}^{(t)} = \tanh(W^{(c)}[h^{(t-1)}, X^{(t)}] + b^{(c)}) \\ C^{(t)} = \Gamma_f^{(t)} \cdot C^{(t-1)} + \Gamma_u^{(t)} \cdot \tilde{C}^{(t)} \\ \Gamma_o^{(t)} = \delta(W^{(o)}[h^{(t-1)}, X^{(t)}] + b^{(o)}) \\ h^{(t)} = \Gamma_o^{(t)} \cdot \tanh(C^{(t)}), \end{cases} \quad (4)$$

where  $\Gamma_f^{(t)}$ ,  $C^{(t)}$  and  $h^{(t)}$  denote the forget gate, the input gate, and the output gate, respectively, while  $W$  and  $b$  represent the weight and the bias factors of different structures, respectively. Furthermore,  $\delta$  denotes sigmoid activation function.

2) *Attention layer*: Attention model (AM) was first introduced from the machine translation task and has become a popular neural network concept [40]. Attention can integrate related information and allow the model to provide dynamic attention to some useful input information, which has been utilized as a useful tool to improve the performance of LSTM network.

We assume that the output of the  $j^{th}$  time step in the  $i^{th}$  layer is  $h_j^i$  ( $i = 1, 2, j = 1, \dots, q$ )

$$z^i = \sum_{j=1}^q a_j^i h_j^{i-1}, \quad (5)$$

where  $a_j^i$  is the attention weight. It can be given by

$$a_j^i = \frac{\exp(e_j^i)}{\sum_{j=1}^q \exp(e_j^i)}, \quad (6)$$

where  $e_j^i$  is the aggregation state.  $e_j^i$  can be obtained via utilizing the Bahdanau-attention method [40]

$$e_j^i = V^T \tanh(W_u \mathbf{S} + W_h h_{j-1}^i), \quad (7)$$

where  $V, W_u$  and  $W_h$  are the input weights, and  $\mathbf{S} = [h_1^{i-1}, \dots, h_q^{i-1}]$  is the output of the  $(i-1)^{th}$  LSTM layer.

Finally, we use the combination of the attention model output  $z^i$  and the LSTM output  $[h_1^{i-1}, \dots, h_q^{i-1}]$  as the input data for the second LSTM layer, i.e.,  $\text{concat}(z^i, h_1^{i-1}, \dots, h_q^{i-1})$ .

3) *Output layer*: The extracted features in the last LSTM layer go through a fully connected layer to obtain the output  $X^{(q+1)}$ . Note that, the output  $X^{(q+1)}$  may not be an integer, and we should round  $X^{(q+1)}$  after prediction.

#### IV. SYSTEM ANALYSIS

The proposed random access scheme aims to satisfy different communication requirements of URLLC and mMTC devices, i.e., high reliability and low access latency for URLLC devices and massive access for mMTC devices.

Based on the predicted number of active URLLC devices, the BS determines the parameters of the multi-user detection algorithm to ensure the reliability requirement. The coding and modulation schemes can be adjusted to satisfy the reliability requirement of URLLC devices based on the number of active URLLC devices [34]–[36]. If the predicted number of URLLC devices is less than the actual value, we assume that all URLLC devices cannot be successfully decoded due to the incorrect coding and modulation schemes. Fig. 4 will show that the probability of such an event, denoted by  $P_{\text{LSTM}}$ , is really small. Thus, the proposed random access scheme can ensure the reliability and access latency requirements of URLLC devices. Therefore, in this section, we only focus on the number of successful access devices, which is given by

$$N^s = N_{\text{U}}^s + N_{\text{M}}^s, \quad (8)$$

where  $N_{\text{U}}^s$  and  $N_{\text{M}}^s$  are the number of successful URLLC devices and mMTC devices, respectively.

For the active URLLC devices, we assume that, if the predicted number of active URLLC devices is less than the real value, all active URLLC devices cannot be successfully decoded. Then, we have

$$N_{\text{U}}^s = N_{\text{U}}(1 - P_{\text{LSTM}}). \quad (9)$$

It is hard to derive the expression of  $P_{\text{LSTM}}$  since the number of active URLLC devices is predicted by an attention-based LSTM prediction model. However, we can compute the expected value though Monte Carlo simulations. Next, we discuss how to derive the term  $N_{\text{M}}^s$  in (8).

Let  $P_{N_{\text{M}}}^u$  denote the probability of  $u$  devices selecting the same preamble among  $N_{\text{M}}$  devices.  $u$  follows a

binomial distribution  $u \sim \mathcal{B}(N_{\text{M}}, \frac{1}{\tau_{\text{M}}})$ , and  $P_{N_{\text{M}}}^u$  is given by

$$P_{N_{\text{M}}}^u = \binom{N_{\text{M}}}{u} \left(\frac{1}{\tau_{\text{p}}}\right)^u \left(1 - \frac{1}{\tau_{\text{p}}}\right)^{N_{\text{M}}-u}. \quad (10)$$

Let  $P_u^t$  denote the probability that  $t$  resource blocks are allocated to these  $u$  devices, i.e.,  $t$  devices experience no TA collision among these  $u$  devices. Let  $N_{u,t}^s$  denote the number of successful devices when  $u$  devices are allocated  $t$  resource blocks. Then,  $N_{\text{M}}^s$  is computed by

$$N_{\text{M}}^s = \tau_{\text{M}} \sum_{u=1}^{N_{\text{M}}} \sum_{t=1(t \neq u-1)}^u N_{u,t}^s P_u^t P_{N_{\text{M}}}^u. \quad (11)$$

Next, we present how to compute terms  $P_u^t$  and  $N_{u,t}^s$  in (11) in detail.

##### (1) $P_u^t$ computation

$P_u^t$  denotes the probability that  $t$  resource blocks can be allocated to  $u$  devices. This means that,  $t$  devices have unique TA values out of  $u$  devices, and, among the remaining  $u-t$  devices, each device has the same TA value as at least one other device. Therefore, to compute the value of  $P_u^t$ , we first need to find cases of each device has the same TA value as at least one other device among the remaining  $u-t$  devices, and then derive TA values allocation ways for each case. The details are described as follows.

Finding such cases is equivalent to finding sets where each element (represents the number of UEs having the same TA value) is larger than 1 and the sum of elements equals  $u-t$ , which is given by

$$\begin{aligned} \text{Find } \mathbf{S} &= [\mathbf{S}(1), \dots, \mathbf{S}(j), \dots, \mathbf{S}(|\mathbf{S}|)] \\ \text{s.t. } \mathbf{S}(i) &> 1, \\ \sum_{i=1}^{|\mathbf{S}|} \mathbf{S}(i) &= u-t, \end{aligned} \quad (12)$$

where  $\mathbf{S}(j)$  denotes the  $j^{th}$  element in set  $\mathbf{S}$ , and  $|\mathbf{S}|$  represents the number of different TA values.

Let  $N_{u-t}$  denote the number of sets satisfying constraints in (12), and  $\mathbf{S}_{u-t}^i$  denote the  $i^{th}$  set. For the case of  $u-t=1$ , it is easy to derive that  $\mathbf{S}_1^i$  is an empty set; for the case of  $u-t=2$ , it is easy to derive that  $N_2=1$  and  $\mathbf{S}_2^1=[2]$ ; for the case of  $u-t=3$ , it is easy to derive that  $N_{u-t}=1$  and  $\mathbf{S}_3^1=[3]$ ; for the case of  $u-t \geq 4$ , sets satisfying constraints in (12) are derived via a recursive method, which is shown in Algorithm 1.

For the  $i^{th}$  set  $\mathbf{S}_{u-t}^i$ , since  $t$  devices have unique TA values and the remaining  $u-t$  devices have  $|\mathbf{S}_{u-t}^i|$  different TA values among  $u$  devices, the total number of different TA values among these  $u$  devices is  $N_{\text{TA}}^i = |\mathbf{S}_{u-t}^i| + t$ . Since there are  $\zeta$  different TA values in the cell (i.e.,  $\text{TA}_1, \dots, \text{TA}_{\zeta}$ ), there are  $N_{\text{TAC}}^i = \binom{\zeta}{N_{\text{TA}}^i} N_{\text{TA}}^i!$

---

**Algorithm 1:** Recursive method of deriving sets satisfying constraints in (12) when  $u - t \geq 4$

---

**Input :**  $N_2, N_3, [S_2^1, \dots, S_2^{N_2}], [S_3^1, \dots, S_3^{N_3}]$   
**Output:**  $\mathcal{D} = [S_{u-t}^1, S_{u-t}^2, \dots, S_{u-t}^{N_{u-t}}], N_{u-t}$

- 1  $\mathcal{C} = \phi, \mathcal{D} = \phi, S_{u-t}^1 = [r];$
- 2  $\mathcal{C} = \mathcal{C} \cup S_{u-t}^1;$
- 3 **for** all  $a \in \{2, \dots, \lceil r/2 \rceil\}$  **do**
- 4      $b = (u - t) - a;$
- 5      $\mathcal{A} = [S_a^1, \dots, S_a^{N_a}], \mathcal{B} = [S_b^1, \dots, S_b^{N_b}];$
- 6     **Combine each element in  $\mathcal{A}$  with each element in  $\mathcal{B};$**
- 7     **for** all  $i \in \{1, \dots, N_a\}, j \in \{1, \dots, N_b\}$  **do**
- 8          $\mathcal{C} = \mathcal{C} \cup [S_a^i, S_b^j];$
- 9     **end**
- 10 **end**
- 11  $\mathcal{D} = [S_{u-t}^1, S_{u-t}^2, \dots, S_{u-t}^{N_{u-t}}] \leftarrow$  Regard sets in  $\mathcal{C}$  having the same elements but in different order as one set;

**Return:**  $\mathcal{D} = [S_{u-t}^1, \dots, S_{u-t}^{N_{u-t}}], N_{u-t} = |\mathcal{D}|$

---

different TA allocation ways if  $\zeta \geq N_{\text{TAC}}^i$ . Otherwise,  $N_{\text{TAC}}^i = 0$ . Then, we have

$$P_u^t = \sum_{i=1, N_{\text{TAC}}^i \geq 1}^{N_{u-t}} \sum_{k=1}^{N_{\text{TAC}}^i} N_{\text{do}} \prod_{g=1}^{N_{\text{TA}}^i} (P_{k_g^i})^{S_{u-t}^i(g)} \prod_{c=N_{\text{TA}}^i+1}^{N_{\text{TA}}^i+t} P_{k_c^i}, \quad (13)$$

where  $P_{k_g^i}$  is the probability that the TA index of a device is  $k_g^i$  (i.e., the probability that a device is located at the  $(k_g^i)^{\text{th}}$  annulus), which is given by

$$P_{k_g^i} = \begin{cases} \int_{\frac{d(k_g^i-1)}{2}}^{\frac{2dk_g^i}{2}} \frac{2x}{R^2} dx = \frac{d^2(2k_g^i-1)}{4R^2}, & k_g^i = 1, \dots, \zeta - 1, \\ \int_{\frac{d(k_g^i-1)}{2}}^R \frac{2x}{R^2} dx = 1 - \frac{d^2(k_g^i-1)^2}{4R^2}, & k_g^i = \zeta, \end{cases} \quad (14)$$

and  $N_{\text{do}}$  stands for the order of these  $u$  devices, which is given by

$$N_{\text{do}} = \frac{\binom{u}{t} (S_{u-t}^i(1)) \prod_{d=2}^{|S_i|} \binom{u - \sum_{r=1}^{d-1} S_{u-t}^i(r)}{S_{u-t}^i(d)}}{\prod_{j=1}^{|\mathcal{D}_i|} c_j^j!}, \quad (15)$$

where  $\mathcal{D}_i$  represents a set consisting of different elements in  $S_{u-t}^i$  and  $c_j^j$ ,  $j = 1, \dots, |\mathcal{D}_i|$  denotes the number of times that the  $j^{\text{th}}$  element of  $\mathcal{D}_i$  appears in set  $S_{u-t}^i$ .

(2)  $N_{u,t}^s$  computation

Based on the procedure of our proposed random access scheme,  $u$  devices selecting the same preamble

are allocated  $t$  resource blocks. On each resource block, only one device has the highest power level. Thus, these  $t$  devices can successfully access the network based on the SIC algorithm in power domain. The remaining  $u-t$  devices first randomly select their resource blocks from these  $t$  resource blocks, and then randomly select their power levels from  $L-1$  available power levels. Let  $N_{u-t}^s$  denote the number of successful devices among the remaining  $u-t$ . Then,  $N_{u,t}^s$  can be written as

$$N_{u,t}^s = t + N_{u-t}^s. \quad (16)$$

Next, we discuss how to derive  $N_{u-t}^s$ .

Let  $P_i$  denote the probability of  $i$  devices selecting the same resource block among these  $u-t$  devices. Apparently,  $i$  follows a binomial distribution of  $i \sim \mathcal{B}(u-t, \frac{1}{t})$ , i.e.,  $P_i = \binom{u-t}{i} (\frac{1}{t})^i (1-\frac{1}{t})^{u-t-i}$ . Let  $P_i^s$  denote the probability that one device can be successfully decoded via the SIC algorithm for the remaining  $u-t$  devices. Then, we have

$$N_{u-t}^s = \sum_{i=1}^{u-t} i \times t \times P_i^s \times P_i. \quad (17)$$

Based on the principle of the SIC algorithm in power domain, in each resource block, the following two events ensure that device selecting power level  $l$  can be successfully decoded: 1) this device is free from power level collision and devices with power levels larger than this device are successfully decoded; 2) this device is free from power level collision and the number of devices with power levels larger than this device is zero. Let  $N_{\text{E1},l}^s$  and  $N_{\text{E2},l}^s$  denote the cases of the first event and the second event, respectively. Apparently,  $N_{\text{E2},l}^s = (L-2)^{i-1}$  and the total number of cases selecting power level is  $(L-1)^i$ . Then,  $P_i^s$  is given by

$$P_i^s = \frac{\sum_{l=1}^{L-1} [N_{\text{E1},l}^s + N_{\text{E2},l}^s]}{L^i} = \frac{\sum_{l=1}^{L-1} \left[ \sum_{j=1}^{l-1} \binom{i-1}{j} \binom{l-1}{j} j!(L-1-l)^{i-j-1} + (L-1-l)^{i-1} \right]}{(L-1)^i}. \quad (18)$$

## V. NUMERICAL RESULTS

In the following, we first present the performance of the attention-based LSTM prediction model, and then make a comparison between our proposed LSTMH-RA scheme and the random access proposed in [23] in terms of the number of successful access devices.



TABLE II  
SIMULATION PARAMETERS

Parameter	Value
$\lambda$ (Mean value of Poisson distribution)	4~8
$d$ (The quantized unit)	156 $m$
$T_s$ (the basic time unit)	$3.072 \times 10^{-7}$ $s$
$c$ (The speed of light)	$3 \times 10^8$ $m/s$
$R$ (The radius of cell)	624, 1000, 1500 $m$
$\tau_p$ The number of preambles	28 ~ 64
$N_M$ (The number of active mMTC devices)	100
$L$ (The number of power levels)	3 ~ 7
$M$ (The number of antennas)	128
$N_a$ (The number of active UEs during one random access procedure)	15 ~ 50
$N_{ij}$ (The number of active URLLC devices)	5

### A. The performance of the attention-based LSTM prediction model

For the attention-based LSTM prediction model, we set the learning rate to 0.001, and utilize the root-mean square loss function. As in [41], we assume that the number of active URLLC devices in each random access time slot has a distribution of  $\mathcal{P}(\lambda)$  where  $\lambda$  is the mean value.

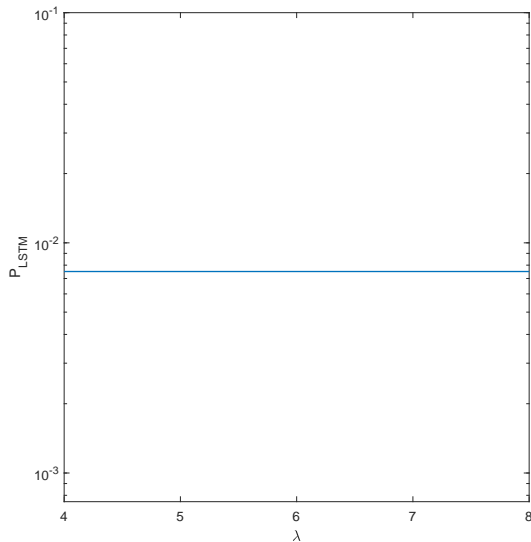


Fig. 4. The probability of the predicted number of active URLLC being less than the actual value.

If the predicted number of URLLC devices is less than the actual value, we assume that all URLLC devices cannot be successfully decoded due to the incorrect coding and modulation schemes. To ensure the reliability and latency requirements of URLLC devices, we take the maximum number of active URLLC devices from  $t$  to  $t + 5$  random access time slots as the possible value in the  $t^{th}$  random access time slot, and set the length of input be equal to  $q = 5$ .

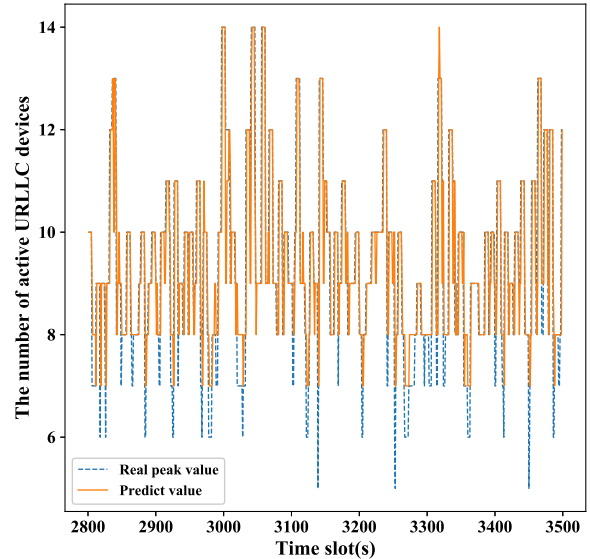


Fig. 5. Prediction results.

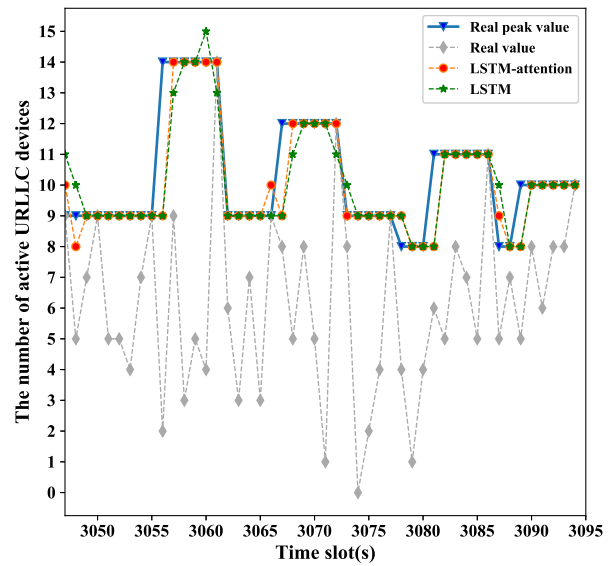


Fig. 6. Prediction comparison.

Fig. 4 shows how the probability  $P_{\text{LSTM}}$  changes with different arrival rates  $\lambda$  ranging from 4 to 8. We see from this figure that,  $P_{\text{LSTM}}$  takes small and almost the same values for different arrival rates  $\lambda$ . This means that our proposed prediction model can ensure the reliability and latency requirements of URLLC devices with high probability. This indicates that the allocated code and modulation parameters can ensure the reliable communication of almost all active URLLC devices. In addition, for the case where the predicted number of URLLC devices is less than the actual value, the BS will allocate multiple resource blocks to these active URLLC devices in the next random access time slot to ensure all active URLLC devices can be decoded successfully within two random access time slots to satisfy the access latency requirement. Thus, the proposed random access scheme can ensure the reliability and access latency requirements of URLLC devices.

Fig. 5 shows the prediction results when we consider multiple random access time slots, where we set  $\lambda$  to 6. The ‘real peak value’ in this figure refers to the maximum number of active URLLC devices from  $t$  to  $t + 5$  random access time slots. We can see from this figure that, the predicted value is very close to the actual value, which indicates that the prediction model is efficient to predict the maximum number of active URLLC devices from  $t$  to  $t + 5$  random access time slots. In addition, for the case where the predicted number of URLLC devices is less than the actual value, the BS will allocate multiple resource blocks to these active URLLC devices in the next random access time slot to ensure all active URLLC devices can be decoded successfully within two random access time slots to satisfy the access latency requirement. Thus, the proposed random access scheme can ensure the reliability and access latency requirements of URLLC devices.

Fig. 6 compares the prediction performance between the proposed attention-based LSTM and basic LSTM prediction model, where we set  $\lambda$  to 6. The LSTM prediction model is obtained by deleting the attention model from our attention-based LSTM model. Furthermore, ‘real value’ is the number of URLLC devices in the  $t^{\text{th}}$  random access time slot. The experimental results show that, compared to the basic LSTM prediction model, our proposed attention-based LSTM prediction model can achieve better performance.

### B. The performance of the proposed LSTMRH-RA

In the simulations, we consider the urban micro scenario and all devices are uniformly distributed in the cell. In addition, the quantized unit is  $d = 16T_s c = 156 m$  where  $T_s = 3.072 \times 10^{-7} s$  is the basic time unit [42] and  $c = 3 \times 10^8 m/s$  is the speed of light.

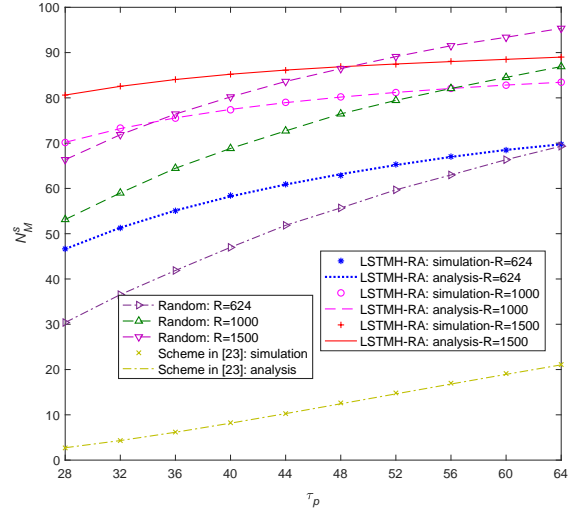


Fig. 7. The number of successful mMTC devices versus the number of preambles.

Fig. 7 shows the number of successful mMTC devices with respect to the number of preambles for different radius of cell. We set the radius of cell to 1500, 1000, and 624, the number of active mMTC devices to 100, power levels to 3, and the number of antennas at the BS to 128. In addition, to demonstrate the advantage of the power allocation strategy utilized in the proposed LSTMH-RA scheme, we consider a scheme which allows each device to select its uplink transmit power randomly and uniformly. This scheme is termed ‘Random’ in Fig. 7. We observe that, for different radius, with the decrease of the number of preambles (i.e., the number of devices selecting the same preamble increasing), the gap between the proposed LSTMH-RA scheme and the Random scheme increases. This indicates that the proposed LSTMH-RA scheme is more robust to the Random scheme for the crowded scenarios. We also see from Fig. 7 that, with the increase of the number of preambles, the number of successful mMTC devices increases and is significantly higher than that of the random access scheme proposed in [23]. Furthermore, with the increase of the size of the cell, the number of successful mMTC devices increases. The reason is that, with the increase of the size of the cell, the number of different TA values increases and thus the BS can distinguish more mMTC devices.

Fig. 8 shows the number of successful mMTC devices with respect to the number of power levels for different radius of cell. We set the radius of cell to 1500, 1000, and 624. We set the number of active mMTC devices to 100, the number of preambles to 28, and the number of antennas at the BS to 128. We can see from Fig. 8 that, with

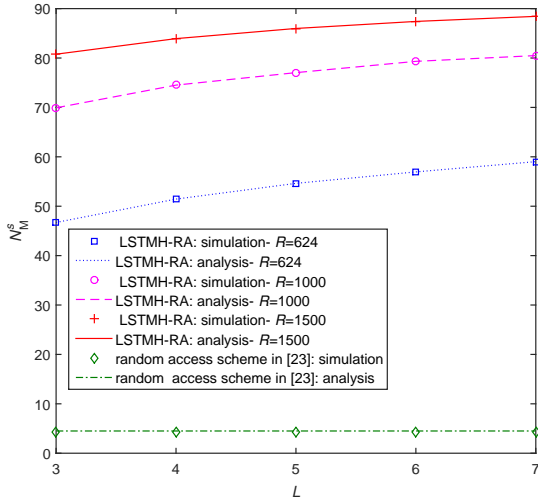


Fig. 8. The number of successful mMTC devices versus the number of power levels.

the increase of the number of power levels, the number of successful mMTC devices increases and is significantly higher than that of the random access scheme proposed in [23]. Furthermore, with the increase of the size of the cell, the number of successful mMTC devices increases. The reason is the same as we described in Fig. 7.

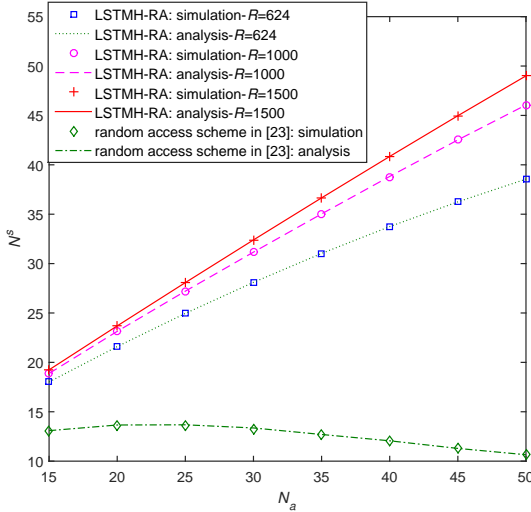


Fig. 9. The number of successful devices versus the number of active devices.

Fig. 9 shows how the number of successful devices changes with the number of active devices. We set the radius of cell to 1500, 1000, and 624, the number of preambles to 28, the number of antennas at the BS to 128, and the number of power levels to 3. Among these

active devices, the number of active URLLC devices is set to 5 and these active URLLC devices belong to different groups, and thus the number of preambles allocated to the URLLC devices is 23 in the random access scheme proposed in [23]. Based on Fig. 4, we can see that  $P_{LSTM}$  in (9) is about  $7.5 \times 10^{-3}$ . We can see from Fig. 9 that, with the increase of the number of active devices, the number of successful devices increases and is significantly higher than that of the random access scheme proposed in [23]. Furthermore, with the increase of the size of the cell, the number of successful mMTC devices increases. The reason is the same as we described in Fig. 7.

## VI. CONCLUSION

In this paper, an LSTMH-RA scheme has been proposed to support diverse QoS requirements in 6G MTC networks where URLLC and mMTC devices coexist. To meet URLLC devices' latency and reliability access requirements, this scheme employs a proposed attention-based LSTM prediction model to predict the number of active URLLC devices, and thus URLLC devices can access the network via a two-step contention-free access procedure. In addition, to meet mMTC devices' massive access requirement, mMTC devices access the network via a contention-based TA-aided access mechanism. Numerical results have shown that, compared with the existing schemes, the LSTMH-RA scheme significantly improves the successful access probability, and satisfies the diverse QoS requirements of URLLC and mMTC devices.

## REFERENCES

- [1] H. Song, J. Bai, Y. Yi, J. Wu, and L. Liu, "Artificial intelligence enabled internet of things: Network architecture and spectrum access," *IEEE Computational Intelligence Magazine*, vol. 15, no. 1, pp. 44–51, 2020.
- [2] R. Atat, L. Liu, J. Wu, J. Ashdown, and Y. Yi, "Green massive traffic offloading for cyber-physical systems over heterogeneous cellular networks," *Mobile Networks and Applications*, vol. 24, no. 4, pp. 1364–1372, 2019.
- [3] P. Popovski, V. Braun, and e. a. H.-P. Mayer, "D1.1: Scenarios, requirements and KPIs for 5G mobile and wireless system," document ICT-317669-METIS, Tech. Rep., Apr. 2013.
- [4] G. Flagship, "Key drivers and research challenges for 6G ubiquitous wireless intelligence," University of Oulu, Tech. Rep., 2019.
- [5] K. David and H. Berndt, "6G vision and requirements: Is there any need for beyond 5G?" *IEEE Transactions on Vehicular Technology*, vol. 13, no. 3, pp. 72–80, Sep. 2018.
- [6] E. C. Strinati, S. Barbarossa, J. L. Gonzalez-Jimenez, D. Kténas, N. Cassiau, and C. Dehos, "6G: The next frontier," *arXiv preprint arXiv:1901.03239*, 2019.
- [7] C. VNI, "Cisco visual networking index: Forecast and trends, 2017-2022," *White Paper*, 2018.
- [8] N. H. Mahmood, H. Alves, O. A. López, M. Shehab, D. P. M. Osorio, and M. Latva-Aho, "Six key features of machine type communication in 6G," in *2020 2nd 6G Wireless Summit (6G SUMMIT)*, 2020, pp. 1–5.

- [9] 3rd Generation Partnership Project, "Study on RAN improvements for machine type communications, TR 37.868," 3GPP, Tech. Rep., v11.0.0, Sep. 2011.
- [10] T. Lin, C. Lee, J. Cheng, and W. Chen, "PRADA: Prioritized random access with dynamic access barring for MTC in 3GPP LTE-A networks," *IEEE Transactions on Vehicular Technology*, vol. 63, no. 5, pp. 2467–2472, Jun. 2014.
- [11] L. Ferdouse and A. Anpalagan, "A dynamic access class barring scheme to balance massive access requests among base stations over the cellular M2M networks," in *2015 IEEE 26th Annual International Symposium on Personal, Indoor, and Mobile Radio Communications (PIMRC)*, Aug. 2015, pp. 1283–1288.
- [12] S. Lien, T. Liao, C. Kao, and K. Chen, "Cooperative access class barring for machine-to-machine communications," *IEEE Transactions on Wireless Communications*, vol. 11, no. 1, pp. 27–32, Dec. 2012.
- [13] Z. Wang and V. W. S. Wong, "Optimal access class barring for stationary machine type communication devices with timing advance information," *IEEE Transactions on Wireless Communications*, vol. 14, no. 10, pp. 5374–5387, Oct. 2015.
- [14] A. Laya, L. Alonso, and J. Alonso-Zarate, "Is the random access channel of LTE and LTE-A suitable for M2M communications? a survey of alternatives," *IEEE Transactions on Wireless Communications*, vol. 16, no. 1, pp. 4–16, 2014.
- [15] J.-B. Seo, H. Jin, and B. C. Jung, "Multichannel uplink NOMA random access: Selection diversity and bistability," *IEEE Communications Letters*, vol. 23, no. 9, pp. 1515–1519, Sep. 2019.
- [16] M. Shirvanimoghaddam, Y. Li, M. Dohler, B. Vucetic, and S. Feng, "Probabilistic rateless multiple access for machine-to-machine communication," *IEEE Transactions on Wireless Communications*, vol. 14, no. 12, pp. 6815–6826, 2015.
- [17] Y. Liang, X. Li, J. Zhang, and Z. Ding, "Non-orthogonal random access for 5G networks," *IEEE Transactions on Wireless Communications*, vol. 16, no. 7, pp. 4817–4831, 2017.
- [18] J. Ahn, B. Shim, and K. B. Lee, "EP-based joint active user detection and channel estimation for massive machine-type communications," *IEEE Transactions on Communications*, vol. 67, no. 7, pp. 5178–5189, Jul. 2019.
- [19] L. Liu and W. Yu, "Massive connectivity with massive MIMO-Part I: Device activity detection and channel estimation," *IEEE Transactions on Signal Processing*, vol. 66, no. 11, pp. 2933–2946, 2018.
- [20] T.-O. Luis, P.-P. Diego, P. Vicent, and M.-B. Jorge, "Reinforcement learning-based ACB in LTE-A networks for handling massive M2M and H2H communications," in *Proceeding of 2018 IEEE International Conference on Communications (ICC)*, 2018, pp. 1–7.
- [21] G. Gui, H. Huang, Y. Song, and H. Sari, "Deep learning for an effective non-orthogonal multiple access scheme," *IEEE Transactions on Vehicular Technology*, vol. 67, no. 9, pp. 8440–8450, 2018.
- [22] N. Ye, X. Li, H. Yu, A. Wang, W. Liu, and X. Hou, "Deep learning aided grant-free NOMA toward reliable low-latency access in tactile internet of things," *IEEE Transactions on Industrial Informatics*, vol. 15, no. 5, pp. 2995–3005, 2019.
- [23] T. N. Weerasinghe, I. A. M. Balapuwaduge, and F. Y. Li, "Preamble reservation based access for grouped mMTC devices with URLLC requirements," in *ICC 2019 - 2019 IEEE International Conference on Communications (ICC)*, 2019, pp. 1–6.
- [24] R. Qi, X. Chi, L. Zhao, and W. Yang, "Martingales-based ALOHA-type grant-free access algorithms for multi-channel networks with mMTC/URLLC terminals co-existence," *IEEE Access*, vol. 8, pp. 37 608–37 620, 2020.
- [25] H. Han, W. Zhai, F. Zhou, L. Liu, J. Wu, N. Zhang, and J. Zhao, "LSTM-aided hybrid random access scheme for 6G machine type communication networks," *arXiv preprint arXiv:2012.13537*, 2021.
- [26] E. Björnson, E. de Carvalho, J. H. Sørensen, E. G. Larsson, and P. Popovski, "A random access protocol for pilot allocation in crowded massive MIMO systems," *IEEE Transactions on Wireless Communications*, vol. 16, no. 4, pp. 2220–2234, Apr. 2017.
- [27] E. Björnson, E. G. Larsson, and T. L. Marzetta, "Massive MIMO: Ten myths and one critical question," *IEEE Communications Magazine*, vol. 54, no. 2, pp. 114–123, 2016.
- [28] X. Li, Y. Li, H. Han, and X. Guo, "A joint SUCR protocol and TA information pilot random access scheme," in *2017 IEEE 86th Vehicular Technology Conference (VTC-Fall)*, 2017, pp. 1–5.
- [29] Z. Wang and V. W. S. Wong, "Optimal access class barring for stationary machine type communication devices with timing advance information," *IEEE Transactions on Wireless Communications*, vol. 14, no. 10, pp. 5374–5387, 2015.
- [30] J. Choi, "Re-Transmission diversity multiple access based on SIC and HARQ-IR," *IEEE Transactions on Communications*, vol. 64, no. 11, pp. 4695–4705, 2016.
- [31] 3rd Generation Partnership Project, "E-UTRA physical channels and modulation, TS 36.211," *IET Communications*, V12.5.0, 2015.
- [32] H. Han, X. Guo, and Y. Li, "A high throughput pilot allocation for M2M communication in crowded massive MIMO systems," *IEEE Transactions on Vehicular Technology*, vol. 66, no. 10, pp. 9572–9576, Oct. 2017.
- [33] 3rd Generation Partnership Project, "R1-167889 3GPP TSG RAN WG1 Meeting, Gothenburg, Sweden," 3GPP, Tech. Rep., 26th Aug. 2016. [Online]. Available: <http://www.3gpp.org/ftp/tsg/WG1R1/TSGR186/Docs>
- [34] X. Wang, C. Liang, L. Ping, and S. ten Brink, "Achievable rate region for iterative multi-user detection via low-cost gaussian approximation," *IEEE Transactions on Wireless Communications*, vol. 19, no. 5, pp. 3289–3303, 2020.
- [35] Y. Cui, W. Xu, Y. Wang, J. Lin, and L. Lu, "Side-information aided compressed multi-user detection for uplink grant-free NOMA," *IEEE Transactions on Wireless Communications*, pp. 1–1, 2020.
- [36] F. Li, Y. Peng, and W. Chen, "Sparse multi-user detection with imperfect channel estimation for NOMA systems under Non-Gaussian noise," *IEEE Wireless Communications Letters*, pp. 1–1, 2020.
- [37] H. Han, X. Zhu, , and Y. Li, "Generalizing long short-term memory network for deep learning from generic data," *ACM Transactions Knowledge Discovery from Data*, vol. 14, no. 2, pp. 1–28, Feb. 2020.
- [38] Y. Wang, M. Huang, L. Zhao, , and X. Zhu, "Attention-based LSTM for aspect-level sentiment classification," in *Conference on Empirical Methods in Natural Language Processing*, Nov. 2016, pp. 606–615.
- [39] K. Greff, R. K. Srivastava, J. Koutník, B. R. Steunebrink, and J. Schmidhuber, "LSTM: A search space odyssey," *IEEE Transactions on Neural Networks & Learning Systems*, vol. 28, no. 10, pp. 2222–2232, 2016.
- [40] D. Bahdanau, K. Cho, and Y. Bengio, "Neural machine translation by jointly learning to align and translate," in *3rd International Conference on Learning Representations, ICLR 2015, San Diego, CA, USA, May 7-9, 2015, Conference Track Proceedings*, 2015.
- [41] M. Alsenwi, N. H. Tran, M. Bennis, S. R. Pandey, A. K. Bairagi, and C. S. Hong, "Intelligent resource slicing for eMBB and URLLC coexistence in 5G and beyond: A deep reinforcement learning based approach," *IEEE Transactions on Wireless Communications*, 2021.
- [42] M. Zhang, Y. Li, and X. Guo, "A novel random access scheme for stationary machine-type communication devices," *IET Communications*, vol. 12, no. 19, pp. 2448–2453, Apr. 2018.